Leukemia (1999) 13, 1592–1600

http://www.stockton-press.co.uk/leu

Cytogenetic analysis of the bipotential murine pre-B cell lymphoma, P388, and its derivative macrophage-like tumor, P388D1, using SKY and CGH

AE Coleman[1], ST Forest[1], N McNeil[2], AL Kovalchuk[1], T Ried[2] and S Janz[1]

[1]*Laboratory of Genetics, Division of Basic Sciences, and* [2]*Genome Technology Branch, National Human Genome Research Institute, National Institutes of Health, Bethesda, MD, USA*

Spectral karyotyping (SKY) and comparative genomic hybridization (CGH) were used to elucidate the divergent cytogenetic make-up of the prototypical bilineage lymphoblastic pre-B lymphoma, P388, and its progenitor macrophage-like tumor, P388D1. P388 was found to be diploid and genomically stable. P388D1 was triploid, highly unstable and characterized by numerous marker chromosomes (Chrs) and composite rearrangements. The karyotype of P388D1 was so complex that its clonal relatedness to P388 would have remained questionable without confirmation by molecular analysis of the clonotypic immunoglobulin heavy-chain and light-chain gene recombinations that coexisted in both tumors. The intrinsic instability of the P388D1 genome was indicated by the observation that only four out of 42 aberrations uncovered by SKY (in a total of 27 metaphases) occurred consistently (100% incidence), whereas 27 changes occurred non-randomly (27 to 96% incidence) and 11 alterations randomly (4 to 11% incidence). Persistent cytogenetic instability was also observed in P388 'macrophages' after phorbol ester- and ionomycin-induced conversion *in vitro* of P388 lymphoma cells. The 'cytogenetic noise' in these cells was manifested by a multiplicity of sporadic chromosomal aberrations; ie 25 distinct changes were identified by SKY in 40 metaphases. The results in P388D1 and P388 'macrophages' were interpreted to indicate that the myeloid differention program in the bipotential pre-B cell lymphoma P388 is invariably characterized by karyotypic instability. The study presented here demonstrates the power of the combined SKY and CGH approach to resolve complicated karyotypes of important and widely used mouse tumors.

Keywords: molecular cytogenetics; bilineage differentiation potential; phorbol ester-induced cytogenetic changes; karyotypic instability

Introduction

P388 is a lymphoblastic lymphoma of pre-B cell origin that was induced in 1955 in a female DBA mouse that had been skin-painted with the genotoxic carcinogen, methylcholanthrene. In 1957, Dawe and Potter[1] described the morphological transition *in vitro* of P388 toward a macrophage-like phenotype and observed that upon injection into mice the macrophage-like cells yielded a malignant macrophage-like tumor, which was named P388D1. This finding has presented an intriguing problem to cellular immunologists ever since; the apparent ability of certain immature B cells to acquire macrophage characteristics in a process that has been termed 'lineage switch', 'lineage infidelity', or 'lineage promiscuity'. The genetic relationship of P388 and P388D1 remained unexplained for nearly 30 years until Bauer *et al*[2] showed by Southern analysis that the two cell lines had similar immunoglobulin gene rearrangements. This result suggested, but did not prove unequivocally, that P388D1 'macrophages' originated from P388 pre-B lymphoma cells.[2] Other examples of bipotential B-lymphocytic tumors that can undergo conversion to cells with properties of macrophages have been reported subsequently.[3–5] More recently, Borrello and Phipps expanded on an earlier lead obtained by Katoh *et al*[6] and produced strong evidence for the existence of a normal nonmalignant counterpart to the malignant B/macrophage cell.[7] In proposing that the normal bilineage B/macrophage may be important for certain forms of Th2-typical immune responses, these authors suggested that the above-described 'lineage switch' may have physiological relevance.

P388 and P388D1 have been distributed all over the world and employed by countless investigators as their principal experimental system. P388 and its various derivative sublines have been utilized extensively as a preclinical cancer model for the screening of new anticancer drugs, the efficacy testing of known cytostatic compounds, and the refinement of radiation therapy against malignant neoplasms (see Refs 8–10 for recent examples). Both historically[11] and in contemporary studies,[12–14] P388D1 has been used by numerous research groups as a prototypical macrophage line. In our laboratory, P388D1 was employed in studies that led to the discovery of the B cell growth factor IL-6.[15] In additional experiments on phagocyte-mediated mutagenicity, it was used as an effector cell that damaged target cell DNA by the release of reactive oxygen intermediates.[16] The widespread use of P388 and P388D1 has always generated considerable interest in the karyotype of the tumors. However, until recently efforts to karyotype P388 and P388D1 were frustrated by the intrinsic limitations of classical G-banding techniques in the mouse. These techniques are notorious for their difficulty and ambiguity when the tumor metaphase plate contains complex rearrangements or marker chromosomes.

The genome-wide molecular cytogenetic screening methods of spectral karyotyping (SKY) and comparative genomic hybridization (CGH) were applied in this study to overcome the limitations of G-banding in determining the complete karytotypes of P388 and P388D1. The analysis revealed a striking contrast between the genomic stability of the two cell lines. The P388 lymphoma was found to be a diploid, remarkably stable tumor, in which approximately half of the chromosome complement was unchanged after more than 40 years of repeated passaging *in vivo* and *in vitro*. In contrast, the P388D1 macrophage-like tumor presented as a triploid, highly unstable line that contained numerous translocations, markers, and only a few chromosomes that were left unaltered. In fact, the genome of P388D1 was so heavily rearranged that the clonal relatedness to P388 was almost completely obscured at the karyotypic level. This situation illustrated the largely divergent cytogenetic evolution of the two cell lines and rendered impossible any attempts to identify the putative genomic event(s) that may have caused the initial switch to the macrophage-typical differentiation program in P388D1.

The data presented here provide a benchmark for the

Correspondence: S Janz, LG, DBS, NCI, Bldg 37, Rm 2B10, Bethesda, MD 20892-4255, USA; Fax: (301)402-1031
Received 9 April 1999; accepted 3 June 1999

cytogenetic comparison of various sublines of P388 and P388D1 that are maintained in many laboratories. Furthermore, the results demonstrate the potency of the combined SKY and CGH approach to resolve complicated karyotypes of important and widely used mouse tumors.

Materials and methods

Cell culture and metaphase preparation

P388 and P388D1 cells have been passaged sporadically in our laboratory for more than 40 years. The cells were cultured in RPMI 1640 containing 10% fetal calf serum, 200 mM L-glutamine and 50 μM 2-mercaptoethanol at 37°C in a humidified atmosphere containing 5% CO_2 in air. The conversion of P388 lymphoma cells to macrophage-like cells was induced by treatment for 3 days with 50 μM TPA (12-*O*-tetradecanoylphorbol-13-acetate) and 500 ng/ml ionomycine[17] followed by 3 more days in culture in the absence of inducing agents. The differentiation process was monitored by assessing the fraction of adherent cells in the culture dish by microscopy, analyzing changes in morphology in Wright's Giemsa-stained cytofuge specimens, determining the production of lysozyme and macrophage-typical esterases, and evaluating the ability of P388 'macrophages' to ingest small latex beads. Metaphase spreads were prepared on day 6 according to standard cytogenetic procedures. Briefly, the cells were subjected to hypotonic treatment in 75 mM KCl for 15 min at ambient temperature, fixed in methanol/acetic acid (3:1, v/v), dropped on to glass slides previously dipped into 70% acetic acid to facilitate spreading of chromosomes, and then air-dried.

SKY analysis

Spectral karyotyping in the mouse, which has been described in detail elsewhere,[18,19] utilizes 20 uniquely labeled chromosome-specific FISH probes, epifluorescence microscopy, digital imaging and Fourier spectroscopy to visualize each chromosome in a different color. Briefly, FISH probes were obtained by flow sorting of individual mouse chromosomes, amplification of the chromosomal DNA by two rounds of degenerate oligonucleotide-primed PCR, and labeling of the generated PCR products in a combinatorial manner with the fluorochromes, Spectrum Orange (dUTP conjugate; Vysis, Downers Grove, IL, USA), rhodamine 110 (Perkin Elmer, Foster City, CA, USA) and Texas Red (12-dUTP conjugate; Molecular Probes, Eugene, OR, USA) or the haptens, biotin-16-dUTP and digoxigenin-11-dUTP (Boehringer Mannheim, Indianapolis, IN, USA). After probe hybridization, biotin was detected by avidin-Cy5 (Amersham, Arlington Heights, IL, USA) and digoxigenin was detected by mouse anti-digoxigenin (Sigma, St Louis, MO, USA) followed by sheep anti-mouse Cy5.5 (Amersham). The chromosomes were counterstained with DAPI and embedded in an antifade solution containing 1,4-phenylenediamine (Sigma). Spectral images were acquired on a Leica DMRBE epifluorescence microscope equipped with a SD200 SpectraCube (Applied Spectral Imaging, Carlsbad, CA, USA) and a customized tripple bandpass optical filter (SKY1; Chroma Technology). Spectrum-based classification of the raw spectral images was performed using the software Sky View (Applied Spectral Imaging). DAPI-banded grey scale images of the same cells were captured separately, electronically inverted and contrast enhanced using the same software.

CGH analysis

Comparative genomic hybridization, described in detail elsewhere,[20,21] can be used to detect gains and losses in the average mouse tumor genome. CGH was performed on lymphoblast metaphases prepared from the spleen of 4- to 6-week-old female C57BL/6 mice after *in vitro* culture of splenocytes with LPS (25 μg/ml) for 48 h. Genomic DNA was isolated by a standard extraction method using phenol and chloroform. The control genome (liver) and the tumor genome (P388 or P388D1) were differentially labeled by nick translation with digoxigenin-11-dUTP and biotin-16-dUTP (Boehringer Mannheim), respectively. The immunochemical detection of the biotinized probe was performed by two incubations with avidin-FITC (Vector Laboratories, Burlingame, VT, USA). The digoxigenin-labeled probe was detected with a mouse anti-digoxigenin antibody (Sigma) followed by two successive incubations with polyclonal antibodies conjugated with TRITC (Sigma). Chromosomes were counterstained with DAPI and covered in 1,4-phenylenediamine antifade solution. Images were acquired with a cooled CCD camera (CH250, Photometrics, Tucson, AZ, USA) mounted on a Leica DMRBE epifluorescence microscope (Leica, Wetzlar, Germany). Three exposures were taken, one each for DAPI, FITC and TRITC, using three aligned filters (TR1, TR2, TR3; Chroma Technology, Brattleboro, VT, USA). CGH ratio profiles were calculated with a dedicated software for the mouse that was based upon the previously developed software for human.[22] Chromosomes were identified on the basis of the inverted DAPI-banded images. The average ratio profile was determined as the mean value of 15 metaphase spreads. Detection thresholds were 0.75 and 1.25 for losses and gains of copy numbers, respectively.

PCR analysis of V(D)J rearrangement

B cell typical immunoglobulin (Ig) gene rearrangements common for P388 and P388D1 were detected by direct PCR and further elucidated by DNA sequencing. High-fidelity PCR kits (Boehringer Mannheim) were used to amplify 500 ng aliquots of DNA using a hot start technique and the following cycling conditions: 30 cycles of template denaturation at 95°C for 15 s, primer annealing for 20 s at 62°C and primer extension at 68°C for 4 min in the first cycle with a progressive prolongation of the extension time by 20 s for each of the subsequent cycles. PCR products were fractionated on agarose gels, stained with ethidium bromide, gel purified using the QIAquick gel extraction kit (Qiagen, Valencia, CA, USA), and sequenced directly using the Femtomole cycle sequencing kit (Promega, Madison, WI, USA). To exclude artifacts, recombinational fragment were PCR amplified and sequenced at least twice. PCR primers had the following designations and sequences, 5′ to 3′: V_H 7183, gcg-aag-ctt-gtg-gag-tct-ggg-gga-ggc-tta; V_HJ558, gcg-aag-ctt-aa/gg-ctt-ggg-a/gct-tca-gtg-aag; 5′J_H4, ccc-act-cca-ctc-ttt-gtc-cct-atc; 5′J_H3, gga-ttc-tga-gcc-ttc-agg-acc-aa; LINE-1, gct-gcg-ttc-tga-tga-tgg-tga-gtg; V_κ23, g/aa/gc-a/gtt-g/ct/ag-atg-a/tca-cag-tct/g-cca; 5′J_κ5, gac-act-gta-tgc-cac-gtc.[23–25]

Results

SKY in P388

The SKY analysis of the P388 lymphoma was based on a total of 26 metaphase cells that were completely evaluated. It generated a complete, consistent karyotype that is summarized in Table 1 and illustrated in Figure 1. P388 cells were diploid with a modal chromosome number of 39 and a single Robertsonian chromosome, T(2;4)Rb(2,3), present in all cells (Figure 1, second row, center). Three reciprocal translocations were identified, the T(1;13), T(2;4), and T(11;18). One product of the T(2;4), Chr T(2;4), apparently had undergone a secondary Robertsonian translocation with Chr 3 to create the above-mentioned tripartite chromosome, T(2;4)Rb(2,3). Additional aberrations included: (1) three non-reciprocal translocations,

Table 1 Summary of chromosomal aberrations in P388 and P388D1 as detected by SKY and CGH

Chr	*P388 (SKY)*[a]	*P388 (CGH)*[b]	*P388D1 (SKY)*[c]	*Frequency*[d]	*P388D1 (CGH)*[e]
1	T(1;13)	—	Rb(1,1)	27	Gains band A and H
			Rb(Del 1, Del 1)	26	
			Rb(Del 1, Del 1)T(Del 1;2)	1	
2	T(2;4)Rb(2,3)	—	T(2;10)	26	Gain E-H
			Del 2	24	(most significantly H3)
			Rb(Del 2, Del 11)	23	Loss A3-B
			Rb(Del 2,13)	19	
			Rb(Del 2, Del 14)	9	
3	—	—	Del 3 (large)	27	Gain F1-3
			Del 3 (small)	27	Loss A2-C
4	T(4;2)	Loss C4-5	Del 4	27	Loss A2, B1-E
	Del 4				
5	Dup 5	Gain G	Del 5	25	Gain F-G
			T(5;13)Rb(5,19)	22	Loss B
			T(5;6)	7	
6	—	—	T(6;14)Rb(6,16)T(16;10)	26	Gain C1
			T(6;14)	16	Loss G-D1
7	—	—	T(7;15)Rb(7,18)	25	Loss A-C, E3-F
			T(7;12)	24	
			T(7;15)	1	
8	T(8;18)		Rb(8,8)	26	Gain B3-C1
			Del 8	1	
			Rb(8,8)T(8;1)	1	
9	—	—	Is(9;17)T(17;5)Rb(17,6)T(6;5)	26	Gain A-D
			Is(9;17)T(18;5)Rb(17,6)	23	
			Rb(Del 9,12)	21	
10	T(10;16)	—	T(10;16;10;5)	23	Gain A2-3
			Rb(10,12)	20	
11	T(11;18)	—	—	Loss A2-A4	
12	—	—	T(12;19;17; Del 2)Rb(12,10)	1	—
13	T(13;1)	—	T(13;15)	22	—
			Rb(13,13)T[(13;del 2);(13;del 2)]	1	
14	—	—	Is(14,17)	18	Loss A2-B
15	—	—	T(15;5)	25	Gain D2-F
16	—	Gain E	T(16;3;8)Rb(16,Del 16)T(Del 16;Del 16)	20	Loss A1-C3
			T(16;3;8)Rb(16,16)T(16;19)	3	
			T(16;3;8)	2	
			T(16;3;8)Rb(16,16)T(16;2)	1	
			T(16;3;8)Rb(16,16)T(16;8)	1	
			Del 16	1	
17	—	—	T(17;3)	25	Gain B-F1
			T(Dup 17;19)	24	
			T(17;11)	21	
			T(17;18;5)	1	
18	Del 18	Gain 18 (A-B)	T(18;2)	27	—
	T(18;5)				
	T(18;11)				
19	—	—	—	—	
X	1 copy	Loss X	1 copy (27)	Loss X	

[a]Chromosomal aberrations in untreated P388 lymphoma cells that were detected by spectral karyotyping (SKY). The listed changes were observed consistently in all 26 images that were analyzed. All aberrations are illustrated in Figure 1.
[b]Gains and losses of chromosomal material in untreated P388 lymphoma cells that were detected by comparative genomic hybridization (CGH).
[c]Chromosomal alterations in P388D1 detected by SKY. Most of the changes were not found consistently in the 27 images that were analyzed. All aberrations are illustrated in Figure 2.
[d]Number of occurrences of a cytogenetic change detected by SKY in P388D1.
[e]Gains and losses of genomic material in P388D1 detected by CGH.

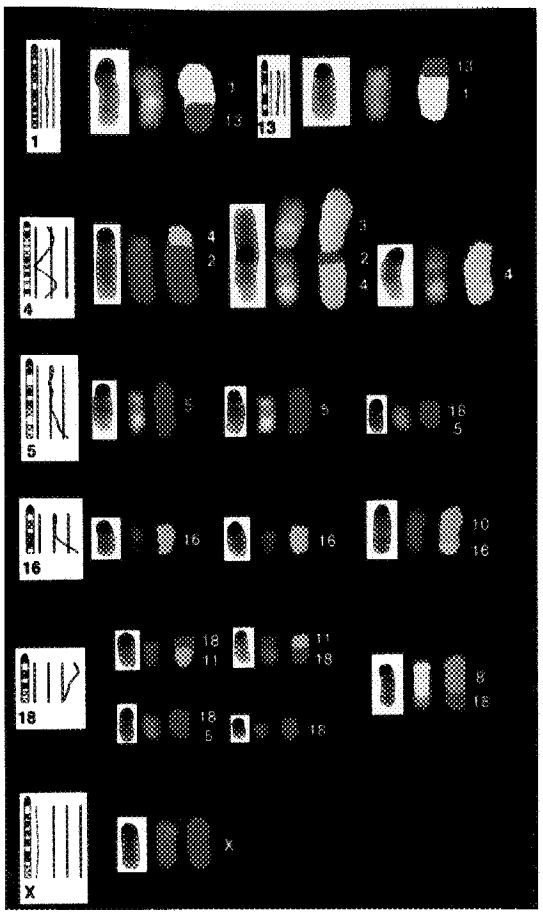

Figure 1 Synopsis of cytogenetic aberrations in P388, as detected by SKY and CGH. Images of aberrant chromosomes are shown in triplets: the inverted gray-scale image of DAPI stained chromosomes are depicted in the white insets to the left, and the painted chromosomes in SKY display colors and SKY classification colors are depicted in the center and to the right, respectively. Ideograms and average CGH ratio profiles of those chromosomes that were found to be altered by SKY are displayed in order from top to bottom at the left margin of the figure, except the ideogram of Chr 13 that is shown in the center of the top row. The three vertical lines to the right of the chromosome ideograms represent the fluorescence ratios between differentially labeled tumor and reference DNA. The left most line indicates a ratio of 0.75, the center line a ratio of 1.0, and the right most line a ratio of 1.25. The irregular, curved lines indicate the CGH ratio profiles. Deviations of these lines to the left of the 0.75-ratio-line and to the right of the 1.25-ratio-line reflect deletions and amplifications in the tumor DNA sample, respectively. The SKY and inverted DAPI images of three reciprocal translocations are shown: T(1;13)(E2;A4 → 5), T(4;2)(A3 → 4;B) and T(11;18)(B;C). One putative product of these translocations, Chr T(2;4), underwent a secondary genetic exchange to produce Chr T(2;4)Rb(2,3), which is illustrated in the center of the second row. Additional SKY and DAPI images include the non-reciprocal translocations T(10;16)(D;C1 → 2), T(18;5)(E1;D3) and T(8;18)(E1;C), the Del18C → D, the Dup5G (shown next to the ideogram of Chr 5), and monosomy X. The copy number losses on Chrs 4C4 → 5 and X, and the copy number gains on Chr 5G, Chr 16E and Chr 18A → B are reflected in the average CGH ratio profiles of the respective chromosomes. Images of unrearranged chromosomes are shown in some cases to facilitate the interpretation of abnormal CGH profiles: one copy of a normal Chr 5 (to the left of Chr T(18;5)), two copies of Chr 16 (to the left of Chr T(10;16)), and one copy (ie the only one) of Chr X (at the bottom). The fact that balanced chromosomal exchanges do not result in gene copy number changes detectable by CGH is illustrated with the assistance of the reciprocal translocation T(1;13) as an example: the corresponding CGH ratio profiles of Chrs 1 and 13 were unchanged.

which produced Chrs T(8;18), T(10;16), and T(18;5); (2) a large deletion in the central portion of Chr 18; (3) a small deletion by genomic standards of Chr 4, which was barely visualized because the resolving power of SKY is limited for detecting deletions; (4) a substantial duplication in the telomeric region of Chr 5; and (5) the apparent loss of one copy of Chr X (ie monosomy X in a tumor that originated in a female mouse). To define the breakpoints of chromosomal rearrangements to a single band/subband or, if the resolution was less accurate, to a region that spanned more than one band, the electronically inverted gray-scale images of the DAPI-counterstained chromosomes were aligned with the spectrally analyzed chromosomes from the same metaphase plate (see the legend to Figure 1 for band designations of chromosomal rearrangements).

CGH in P388

Copy number gains were detected on the distal ends of Chr 5 (band G) and Chr 16 (band C), as well as along the entire length of Chr 18, with an apparent peak at band B (see CGH ratio profiles in Figure 1). Copy number losses were found in the central portion of Chr 4 (band C4→5) and for all of Chr X, which was indicative of its monosomy. Since CGH represents the statistical average of the tumor genome, it was helpful for verifying the recurrent nature of those rearrangements revealed by SKY that resulted in copy number changes (ie all unbalanced exchanges). In addition, CGH was useful for further refining the location of chromosomal breaksites that were previously suggested by SKY. The following three aberrations are examples to illustrate the mutual assistance of SKY and CGH. First, the gains of chromosomal material detected by CGH on Chrs 16 and 18 did not only indicate the recurrent nature of the non-reciprocal translocations, T(10;16) and T(8;18), they were also instrumental in the designation of the corresponding breakpoints on Chrs 16 and 18 to bands C1→2 and E1, respectively. Second, the gain on Chr 5 detected by CGH was not only proof for the recurrence of the duplication of Chr 5, it also helped to narrow the affected region of Chr 5 to the G band. Third, the small deletion of Chr 4 was verified by CGH, shown to be recurrent in nature, and localized to the subbands C4→5. Thus, CGH and SKY appeared to be in remarkably close agreement for the majority of copy number changes found in P388. However, the mutual complementation was not entirely perfect. This was exemplified by the failure of CGH to detect the deletions of the telomeric parts of Chrs 8 and 10 that were postulated to exist because the translocations, T(8;18) and T(10;16), were non-reciprocal in nature. This shortcoming may reflect the fact that CGH tends to detect copy number gains more effectively than losses; deletions typically must amount to 10 Mb or more in order to be reliably detected.[26]

SKY in P388D1

The SKY analysis of the P388D1 macrophage-like tumor was based on a total of 27 thoroughly evaluated metaphase plates (Table 1, Figure 2). P388D1 was triploid in spite of being characterized by a modal chromosome number of 45. A total of 12 chromosomes underwent Robertsonian translocations (centromeric–centromeric fusions), three chromosomes were joined by centromeric–telomeric fusions. If the 15 couplet, fused chromosomes were counted twice and added to the 30

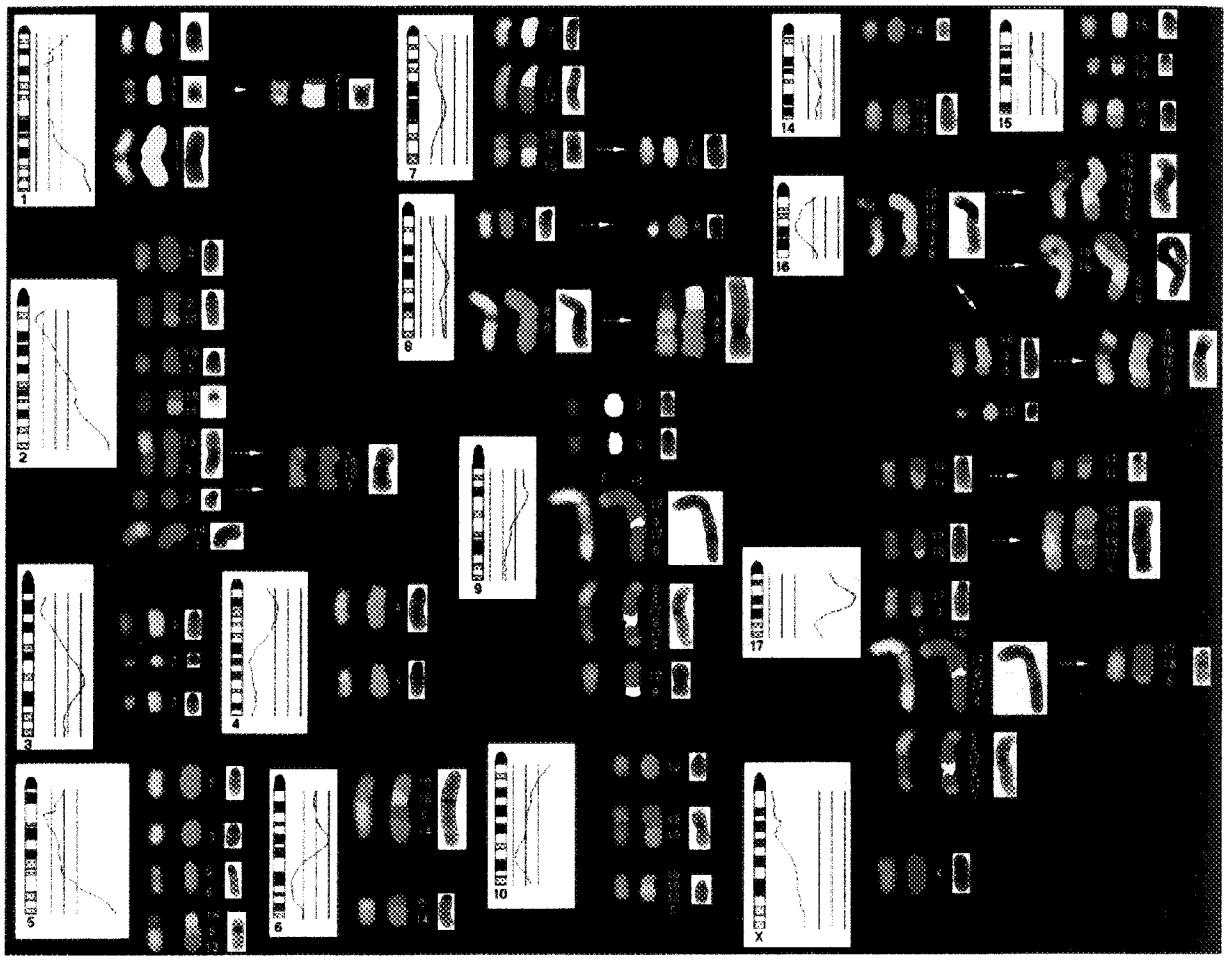

Figure 2 Chromosomal aberrations in P388D1. The same schema used in Figure 1 was employed here to illustrate the cytogenetic changes that were observed in the macrophage-like tumor. The following band desigations for recurrent, non-reciprocal breaksites were determined by the combined SKY, inverted DAPI and CGH analysis: Rb(Del1,Del1)T(Del 1H;2H), T(2H1;10B5 → C1), T(5C → D;13B)Rb(5,19), T(5F;6F1), T(6C2;14A3 → B), Rb(6,16)T((16C;10B);(6D;14A → B)), T(7E → F1;12A1), T(7E → F1;15D), T(7E → F1;15D)Rb(7,19), Rb(8,8)T(8C;1D → E), Is(9;17D → E1)T(18E;5F)Rb(17,6), Is(9;17D → E1)T(17E;5E)Rb(17,6)T(6C → D;5E), T(10B;16;10C → D;5G), Rb(13,13)T((13A-B;del 2E4-F);(13A-B;del 2E4-F)), T(13A2;15E), T(15D;5E), T(16C;3; 8C3 → D2), T(16C;3;8C3 → D2)Rb(16,16)T(16A;2A), T(16C;3;8C3 →D2)Rb(16,16)T(16A;8C3 → D2), T(16C;3;8C3 → D2)Rb(16,16)T(16A;Del16), T(16C;3;8C3 → D2)Rb(16,16)T(16A;19), T(17E2-E5;3F → G), T(17B;11A4 → A5), T(17E;11B), T(17D-E;19C-B), and T(18C;2E → F). Apparent gains of gene copy numbers were localized to Chr 1A, Chr 1H, Chr 2H → E (with a pronounced peak at H3), Chr 3F1 → 3, Chr 5F → G, Chr 6C1, Chr 8B3 → C1, Chr 9A → D, Chr 10A2 → 3, Chr 15D2 → F, and the entire length of Chr 17 with a significant peak at bands B → F1. Apparent losses of copy number gains were found on Chr 2A3 → B, Chr 3A2 → C, Chr 4A2, Chr 4B1 → E, Chr 5B, Chr 6G → D1, Chr 7A → C, Chr 7E3 F, Chr 11A2 → 4 (not shown), Chr 14A2 → B, Chr 16A1 → C3, and along the entire length of Chr X. The precursor-and-product relationships between sporadically occurring, secondarily rearranged chromosomes that were postulated to be derived from recurrent precursor chromosomes (cf Table 1) are indicated by horizontal arrows. For example, the Rb(Del1,Del1)T(1;2), which was thought to be derived from the Rb(Del1,Del1) by a recombination with a Chr 2-derived fragment, is indicated by an arrow in the upper left hand corner of the figure.

individual, non-fused chromosomes, it becomes apparent that P388D1 indeed contained the exact equivalent of 60 chromosomes. Unlike P388, no reciprocal translocations were encountered in P388D1; instead, a large number of non-reciprocal translocations and marker chromosomes was observed. Furthermore, the majority of aberrations identified in P388D1 occurred more or less randomly in contrast to P388, in which all rearrangements were consistent. A total of 27 aberrations in P388D1 were present in seven to 26 metaphases (26–96% incidence), 11 aberrations were found in one to three metaphases (4–11% incidence), and only five aberrations (ie the Rb(1,1), T(18;2), Del 3, another Del 3, and Del 4) occurred consistently in all 27 metaphases. The large number of random karyotypic alterations was interpreted as a reflection of the continuing genomic instability of P388D1.

CGH in P388D1

CGH analysis uncovered a large number of apparent amplifications and deletions spread throughout the genome. Gains of copy numbers were detected on 10 chromosomes (Chrs 1, 2, 3, 5, 6, 8, 9, 10, 15 and 17) and losses of copy numbers were found on nine chromosomes (Chrs 2, 3, 4, 5, 6, 7, 11, 14 and 16). As in P388, only one copy of Chr X was present in P388D1 (Figure 2). the complexity of the P388D1 genome posed severe difficulties (compared to P388) for attempts to reconcile CGH ratio profiles with SKY images. Nevertheless, a meaningful match between CGH and SKY could be established for most chromosomes. For example, the amplifications of Chrs 1, 2 and 17 identified by CGH were explained by the presence of extra copies of these chromosomes (or fragments

thereof) previously detected by SKY. Likewise, the deletions of Chrs 3, 4 and 16 identified by CGH were apparently caused by deletions of these chromosomes (or fragments thereof) previously observed by SKY (see Table 1 and Figure 2 for details). On the other hand, it was not possible to interpret convincingly the nonlinear nature of the CGH profile for the X chromosome. Unlike P388, in which the monosomy X created a CGH ratio curve that was as expected, perfectly linear and exactly parallel to the left of the 0.75 threshold, the same ratio curve in P388D1 showed a non-linear deviation in its distal part. This seemed to signal the existence of additional Chr X-derived material that could not be accounted for by SKY.

Origin of P388D1 from P388 is obscured at cytogenetic level

Due to the extensive genomic rearrangements of the P388D1 'macrophage' tumor, its derivation from P388, a lymphoblastic pre-B cell lymphoma, was almost entirely obscured at the cytogenetic level. Indications for the clonal relatedness between P388 and P388D1 still detectable by SKY seemed to be limited to the fact that both cell lines contained a single copy of Chr X and to the possibility that the Chr T(10;16;10;5) in P388D1 (Figure 2, bottom center) originated by a secondary recombination of the Chr T(10;16) in P388 (Figure 1, fourth row, on the right). Furthermore, the analysis of DAPI-stained chromosomes suggested that the T(18;2) in P388D1 (Figure 2, next to the ideogram of Chr 2) and the T(18;11) in P388 (Figure 1, fifth row) may have utilized the same breakpoint on Chr 18; however, this has not been demonstrated by fine mapping. CGH support for a precursor-and-product relationship between P388 and P388D1 was also scarce: both cell lines showed a partial gain of Chr 5, very similar losses on Chrs 3 and 4, and the chromosome-wide loss of Chr X (monosomy in both tumors). Not only did the complexity of the P388D1 genome obstruct attempts to prove its derivation from P388, it also made it impossible to identify the putative genomic aberration that may have been critical for the original lineage switch in P388D1.

Genetic fingerprints for the derivation of P388D1 from P388

Because of the difficulties encountered using SKY and CGH to demonstrate the common origin of P388 and P388D1, an irreversible genetic fingerprint at the DNA sequence level was chosen to convincingly establish the clonal relationship. The fine structure of the Ig heavy-chain gene rearrangements on Chr 12 and Ig light-chain rearrangements on Chr 6, two reliable markers for clonality in B lymphocytes and their progenitors, was elucidated by PCR analysis. Two heavy-chain typical VDJ fragments were detected in P388. The first one, which was built from a variable gene that belonged to the V_H7183 family, the SP2.10 diversity gene segment and the J_H4 joining gene fragment (Figure 3, fragment 1), was also found in P388D1. The second VDJ fragment, a $V_HJ558/DFL16.1/J_H3$ rearrangement, was present in P388 but not in P388D1 (Figure 3, fragment 2). The analysis of the Ig light-chain gene recombinations was even more informative with respect to clonal relatedness because two rearrangements were found to coexist in P388 and P388D1. The same $V_\kappa23/J_\kappa1$ rearrangement (Figure 3, fragment 4) and the same illegitimate recombination between a genomic repeat (an inverted LINE-1

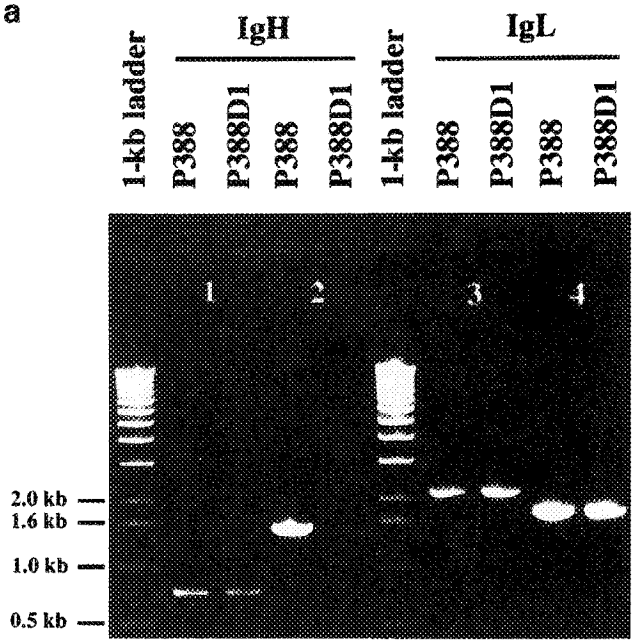

b

Frag.	Rearrangement	Sequence
1	V_H 7183 - SP2.10	tattactgtgcaaga - gataaagggcctata
	SP2.10 - J_H4	aaagggcctatagtc - cctatgctatggact
2	V_H J558 - DFL16.1	gctattactgtgcaa - ttactacggtagtag
	DFL16.1 - J_H3	actacggtagtagct - actggtttgcttact
3	LINE-1 - 5' V_K5	ggagctgaaggggct - acttgatttcaacaa
	V_K5 - J_K5	tcatagttacccacc - cacgttcggtgctgg
4	V_K23 - J_K1	cacagctttcctccg - tggacgttcggtgga

Figure 3 Clonal relatedness of P388 and P388D1. Shown in panel a are PCR products that were separated on an ethidium bromide-stained agarose gel together with a size marker, the 1 kb ladder. A total of four PCR fragments indicative of four distinct B lymphocyte-typical rearrangements of Ig heavy-chain and light-chain genes are depicted. Fragments 1 to 4 were approximately 750 bp, 1.5 kb, 2.1 kb and 1.7 kb long, respectively. The fragments contained the following rearrangements: $V_H7183/SP2.10/J_H4$ (fragment 1), $V_HJ558/DFL16.1/J_H3$ (fragment 2), inverted LINE-1/$V_\kappa5/J_\kappa5$ (fragment 3) and $V_\kappa23/J_\kappa1$ (fragment 4). They were detected with the following primer pairs: V_H7183 and $5'J_H4$ (fragment 1), V_HJ558 and $5'J_H3$ (fragment 2), LINE-1 and $5'J_\kappa5$ (fragment 3) and $V_\kappa23$ and $5'J_\kappa5$ (fragment 4). Fragments 1, 2 and 4 reflected legitimate V(D)J rearrangements that occur during normal B cell development. Fragment 3, however, represented the illegitimate genetic exchange between a repetitive LINE-1 element and the 5' flank of a normal $V_\kappa5/J_\kappa1$ rearrangement. Tabulated in panel b are the 15-bp flanks (5' to 3') of the unique junctions that were determined by DNA sequencing in the corresponding PCR fragment. Tripartite recombinations (fragments 1, 2 and 3) contained two such junctions, while the single bipartite recombination (fragment 4) contained one.

element) and the 5′ flank of a $V_\kappa 5/J_\kappa 5$ rearrangement were observed in P388 and P388D1 (Figure 3, fragment 3). Thus, three immunospecific, clonotypic recombinations were co-detected and found to be indentical by DNA sequencing in both tumors. This result confirmed a previous determination of the clonal relatedness of P388 and P388D1[2] and demonstrated unequivocally that the cell lines were derived from a common precursor cell.

Aberrations in P388 undergoing macrophage-like differentiation

P388 lymphoma cells, like many other bipotential pre-B cell lymphomas, can be induced *in vitro* to differentiate into macrophage-like cells.[27] This was accomplished here by treatment with the phorbol ester, TPA, and the calcium ionophore, ionomycine. The myeloid differentiation program in P388 'macrophages' was monitored by morphological, cytochemical and functional determination of macrophage-typical properties (results not shown). A total of 40 complete, informative metaphases obtained from P388 'macrophages' were analyzed by SKY for the occurrence of chromosomal aberrations that may have accompanied the myeloid lineage switch. The following observations were made. First, P388 'macrophages' consisted of multiple subclones with a ploidy range from hypodiploid (35 Chrs) to hyperhexaploid (122 Chrs). The two most prevalent subclones had modal chromosome numbers of 38 and 39. Second, P388 'macrophages' contained all the aberrations that were seen in P388 lymphoma cells, except one cell in which the P388-typical marker, Rb(2,3)(2;4), was lost (see footnote g to Table 2). Third, the macrophage-like cells were characterized by the highly sporadic occurrence of numerous dicentric, Robertsonian and marker chromosomes that were not seen in untreated P388 cells at the beginning of the cell culture. A total of 25 distinct, sporadic aberrations were observed in 40 metaphases; 24 of them occurred just once and only one was found in three cells. The random nature of these alterations was interpreted to reflect the elevated level of genomic instability in P388 'macrophages'. Fourth, P388 'macrophages' contained one highly recurrent, differentiation-induced aberration, the Is(6;1)T(13;1) (Figure 4, key XVIII). This change was observed in as many as 38 out of 40 metaphases. It most likely originated from an insertion of a small piece of Chr 6 into the Chr 1-derived portion of Chr T(13;1), a hallmark aberration in untreated P388 cells (Figure 1, first row).

Discussion

This paper reports the comprehensive cytogenetic analysis of the prototypical bipotent mouse pre-B cell lymphoma, P388, and its widely known macrophage-like derivative, P388D1. The genomic changes that characterized P388 and P388D1 were detected with the assistance of SKY and CGH, two recently developed genome wide screening methods that have revolutionized the molecular cytogenetics of cancer in human and mouse.[28,29] One important result of this study is the documentation of the remarkable cytogenetic difference between P388 and P388D1. P388 was found to be a genomically stable tumor that harbored a limited number of chromosomal rearrangements. The genomic stability was underlined by the

Table 2 Chromosomal aberrations in P388 'macrophages' that were detected by SKY after treatment with TPA and ionomycin

Cell[a]	Aberration[b]	Key[c]	Cell[a]	Aberration[b]	Key[c]
1	Is(6;1)T(13;1)[1-3][d]	XVIII	28	Endoreduplication	—
	Rb(19,1)T(1;13)	IX	29	T(1;13;19)	XIX
	Double minute[e]	XXVI		Rb(4;15)	I
6	Rb(4;11)[2]	II	30	Rb(1,1)T(1;13)	X
7	Dic 3	XIV	32	Rb(1,18)T(18;11)	XI
8	Rb(5,5)[f]	III	34	Del 15	XXII
10	Is(9;18)	XX		Dic 1	XIII
11	Rb(5,19)	VI		Extra. Elem. 18[i]	XXI
14	Rb(10,14)	V		Extra. Elem. 1[i]	XXII
	Rb(7,9)	IV	35	Dic X	XII
	Del 10	XXIV	38	Rb(14,19)	VIII
15	T(X,16)[g]	XVII	39	Dic 14,15	XVI
18	Dic 10 [3]	XV	40	Rb(7,18)T(18;11)	VII
20	Loss of Rb marker[h]	—			
23	Centromeric piece[e]	XXV			

[a]A total of 40 consecutively numbered P388 'macrophage' metaphase cells were analyzed. Only newly generated aberrations not seen in P388 are listed here.
[b]Chromosomal aberrations detected by spectral karyotyping (SKY). Copy number, if different from one, is indicated in brackets (see metaphases 1, 6 and 18).
[c]Key for looking up the individual aberrations in Figure 3.
[d]Highly recurrent change that was observed in 38 out of 40 images. The copy number of the altered chromosome was associated, by and large, with the ploidy status of the individual cell in which it was observed: it ranged from hypodiploid (35 chromosomes) to hypertriploid (122 chromosomes). The Is(6;1)T(13;1) occurred in a single copy in 25 cells, two copies in 11 cells, and three copies in two cells. It was missing in two cases.
[e]The genomic material present in the double minute was not contained in the SKY probe mix and was, therefore, not classified. The same was true for the centromeric fragment that was found in cell 23 (XXV).
[f]This change was observed in two additional cells, numbers 27 and 36.
[g]Fusion between the centromere of Chr X and the telomere of Chr 16.
[h]The Rb(2,3)T(2;4), a distinct marker chromosome in P388, was present in all P388 'macrophages' except cell 20. It was either lost or broken up and rearranged beyond recognition.
[i]Extrachromosomal elements that did not possess a centromere were distinguished from the shortened 'mini' chromosomes, Del 15 (XXIII) and Del 10 (XXIV), that did contain a centromere.

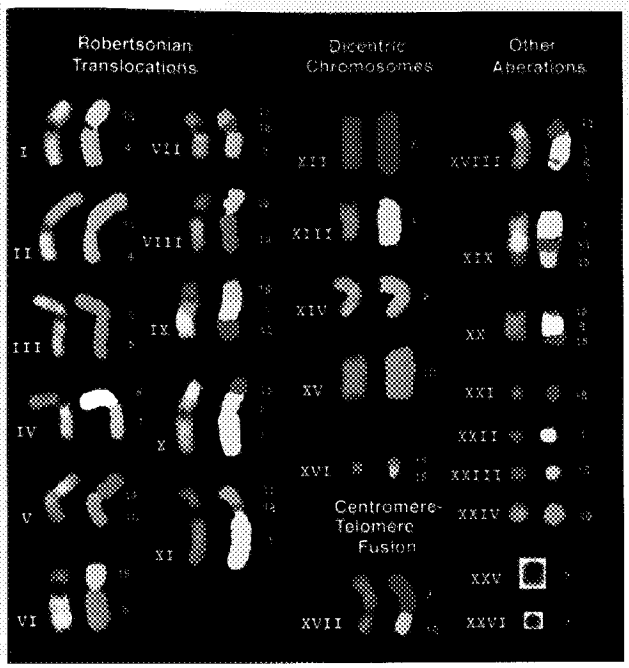

Figure 4 Chromosomal aberrations in P388 'macrophages' after treatment with TPA and ionomycin. SKY revealed the sporadic occurrence of numerous aberrations that included Robertsonian translocations, centromere–telomere fusions, dicentric, composite and marker chromosomes, extrachromosomal elements, and double minutes, as well as other changes (see Table 2 and Results section for details). One chromosome, Is(6;1)T(13;1) (see XVIII at the top right), the putative derivative of Chr T(13;1) (cf Figure 1, top row), was found to be highly recurrent. Two changes, the small centromeric piece (XXV) and the double minute (XXVI), were not visualized by SKY. This was probably caused by the underrepresentation in the SKY probe of the genomic regions contained in these chromosomal fragments; ie sometimes not all genes residing on a particular chromosome are equally amplified during the preparation of SKY probes.

fact that the present karyotype appeared to be very similar to a karyotype obtained 17 years ago.[30] In contrast, P388D1 was characterized by a highly unstable karyotype, whose continuing instability was reflected most impressively by the sporadic appearance of numerous rearrangements of common marker chromosomes. To give but two examples, the Rb(Del1, Del1)T(Del1;2) was the sporadic modification of the Rb(Del1, Del1), which occurred in as many as 26 out of 27 metaphases (see the derivative chromosome indicated by an arrow in Figure 2 to the right of the Chr 1 ideogram). Secondly, four altered and subtly different versions of the common marker chromosome T(16;3;8)Rb(16,Del16)T(Del16;Del16) appeared sporadically in four different tumor cells (see the four derivative chromosomes in Figure 2 to the right of the ideogram of Chr 16). This ongoing karyotypic instability suggests that P388D1 belongs to a group of tumors that are adapted to grow well *in vitro* and *in vivo* in spite of continuing genomic rearrangements. Unstable tumors like P388D1 are of interest for cancer research because they can be used as models for elucidating both the mechanism of karyotypic instability and the tumor cell's adaptability to elevated genomic stress. The possibility to compare an unstable tumor (P388D1) with its stable counterpart (P388), which has been identified unequivocally by the molecular analysis of B cell-typical Ig heavy-chain and light-chain gene rearrangements as the clonally related precursor of P388D1, may offer a particular advantage in this regard.

The utilization of SKY and CGH was hoped to facilitate the understanding of the genomic event that initiated the original lineage switch from P388 to P388D1. This event could be conceptualized as a loss of chromosomal material that contained a gene that is critical for the maintenance of the lymphoblastic phenotype, or a rearrangement that resulted in the activation of a gene that triggers the myeloid differentiation pathway. However, the complexity of the P388D1 genome did not permit the identification of a putative, lineage switch typical rearrangement, and the surrogate *in vitro* experiment of inducing macrophage-like differentiation in P388 cells after treatment with TPA and ionomycin was also not helpful in this respect. Although it is conceivable that the newly formed marker chromosome Is(6;1)T(13;1) – the only differentiation-induced aberration that occurred non-randomly in 38 out of 40 P388 'macrophages' (see XVIII in Figure 4) – may have played a critical role in the switch toward myeloid differentiation, this has not been demonstrated. Other investigators have been more successful and observed highly recurrent, *de novo* generated, composite chromosomes, similar to the Is(6;1)T(13;1), that appeared in P388 sublines resistant to chemotherapeutic drugs.[31,32] Some structural alterations (eg homogenously staining regions) could be associated with a defined molecular change, such as the amplification of the multidrug resistance gene, mdr1. However, the cytogenetic adaptations accompanying drug resistance are likely different from the changes causing a switch in differentiation pattern. Thus, in the absence of gene expression studies in P388 sublines containing the Is(6;1)T(13;1), it cannot be concluded if there is any biological significance of this rearrangement to the lineage switch.

The differentiation of P388 into macrophage-like cells was associated with an acquired genomic instability that was surprisingly intense and mainly reflected by sporadic chromosomal alterations. It is currently not known whether this instability was an intrinsic property of the myeloid differentiation pathway or a consequence of the treatment with TPA, a known clastogen.[33] Experiments with non-clastogenic inducers of myeloid differentiation may help to distinguish between the two possibilities. Moreover, triggering the myeloid differentiation program in P388 transfectants by the overexpression of genes that are known to possess such activities (eg egr-1,[34] v-abl[35] and bcr-abl[36]) may offer an alternative experimental approach to determine the levels of karyotypic instability in cells undergoing macrophage-like differentiation in the absence of exogenously added, chemical compounds. Investigations along this line are in progress in our laboratory. In summary, this study has shown that P388D1 and P388 'macrophages' share the phenotype of increased genomic instability. It has also made it clear that more experiments in P388 will have to be performed and additional bipotent pre-B cell tumors must be studied before it can be decided whether elevated genomic instability is a common feature of the myeloid differentiation program in bilineage tumors.

Acknowledgements

We thank Dr Michael Potter for suggesting this study, sharing his insights on the developmental history of the tumors P388 and P388D1, and making perceptive comments on the experiments. We are grateful to Drs Lynne Rockwood and Fred Mushinski for critical reading of the manuscript and editorial advice. AEC would like to dedicate this paper to the memory of Angel Coleman who will always be missed.

References

1 Dawe A, Potter M. Morphologic and biologic progression of a lymphoid neoplasm of the mouse *in vivo* and *in vitro*. *Am J Pathol* 1957; **33**: 603.
2 Bauer SR, Holmes KL, Morse HC, Potter M. Clonal relationship of the lymphoblastic cell line P388 to the macrophage cell line P388D1 as evidenced by immunoglobulin gene rearrangements and expression of cell surface antigens. *J Immunol* 1986; **136**: 4695–4699.
3 Davidson WF, Pierce JH, Rudikoff S, Morse HC. Relationships between B cell and myeloid differentiation. Studies with a B lymphocyte progenitor line, HAFTL-1. *J Exp Med* 1988; **168**: 389–407.
4 Tanaka T, Wu GE, Paige CJ. Characterization of the B cell-macrophage lineage transition in 70Z/3 cells. *Eur J Immunol* 1994; **24**: 1544–1548.
5 Martin M, Strasser A, Baumgarth N, Cicuttini FM, Welch K, Salvaris E, Boyd AW. A novel cellular model (SPGM 1) of switching between the pre-B cell and myelomonocytic lineages. *J Immunol* 1993; **150**: 4395–4406.
6 Katoh S, Tominaga A, Migita M, Kudo A, Takatsu K. Conversion of normal Ly-1-positive B-lineage cells into Ly-1-positive macrophages in long-term bone marrow cultures. *Dev Immunol* 1990; **1**: 113–125.
7 Borrello MA, Phipps RP. Fibroblasts support outgrowth of splenocytes simultaneously expressing B lymphocyte and macrophage characteristics. *J Immunol* 1995; **155**: 4155–4161.
8 Venkatesan PV, Saravanan K, Nagarajan B. Characterization of multidrug resistance and monitoring of tumor response by combined 31P and 1H nuclear magnetic resonance spectroscopic analysis. *Anticancer Drugs* 1998; **9**: 449–456.
9 Bomgaars L, Gunawardena S, Kelley SE, Ramu A. The inactivation of doxorubicin by long ultraviolet light. *Cancer Chemother Pharmacol* 1997; **40**: 506–512.
10 Labourier E, Riou JF, Prudhomme M, Carrasco C, Bailly C, Tazi J. Poisoning of topoisomerase I by an antitumor indolocarbazole drug: stabilization of topoisomerase I-DNA covalent complexes and specific inhibition of the protein kinase activity. *Cancer Res* 1999; **59**: 52–55.
11 Dawe CJ. Neoplastic properties of animal cell lines. Methods for determining neoplastic properties – discussion. *Natl Cancer Inst Monogr* 1968; **29**: 229–232.
12 Barbour SE, Wong C, Rabah D, Kapur A, Carter AD. Mature macrophage cell lines exhibit variable responses to LPS. *Mol Immunol* 1998; **35**: 977–987.
13 Alicea C, Belkowski SM, Sliker JK, Zhu J, Liu-Chen LY, Eisenstein TK, Adler MW, Rogers TJ. Characterization of kappa-opioid receptor transcripts expressed by T cell and macrophages. *J Neuroimmunol* 1998; **91**: 55–62.
14 Kang JX, Bell J, Leaf A, Beard RL, Chandraratna RA. Retinoic acid alters the intracellular trafficking of the mannose-6-phosphate/insulin-like growth factor II receptor and lysosomal enzymes. *Proc Natl Acad Sci USA* 1998; **95**: 13687–13691.
15 Nordan RP, Potter M. A macrophage-derived factor required by plasmacytomas for survival and proliferation *in vitro*. *Science* 1986; **233**: 566–569.
16 Shacter E, Lopez RL, Beecham EJ, Janz S. DNA damage induced by phorbol ester-stimulated neutrophils is augmented by extracellular cofactors. Role of histidine and metals. *J Biol Chem* 1990; **265**: 6693–6699.
17 Spencker T, Neumann D, Strasser A, Resch K, Martin M. Lineage switch of a mouse pre-B cell line (SPGM-1) to macrophage-like cells after incubation with phorbol ester and calcium ionophore. *Biochem Biophys Res Commun* 1999; **216**: 540–548.
18 Liyanage M, Coleman A, du Manoir S, Veldman T, McCormack S, Dickson RB, Barlow C, Wynshaw-Boris A, Janz S, Wienberg J, Ferguson-Smith MA, Schröck E, Ried T. Multicolour spectral karyotyping of mouse chromosomes. *Nat Genet* 1996; **14**: 312–315.
19 Schröck E, du Manoir S, Veldman T, Schoell B, Wienberg J, Ferguson-Smith MA, Ning Y, Ledbetter DH, Bar-Am I, Soenksen D, Garini Y, Ried T. Multicolor spectral karyotyping of human chromosomes. *Science* 1996; **273**: 494–497.
20 Shi YP, Naik P, Dietrich WF, Gray JW, Hanahan D, Pinkel D. DNA copy number changes associated with characteristic LOH in islet cell carcinomas of transgenic mice. *Genes Chromosomes Cancer* 1997; **19**: 104–111.
21 Weaver ZA, McCormack SJ, Liyanage M, du Manoir S, Coleman A, Schröck E, Dickson RB, Ried T. A recurring pattern of chromosomal aberrations in mammary gland tumors of MMTV-myc transgenic mice. *Genes Chromos Cancer* 1999; **25**: 251–260.
22 du Manoir S, Schrock E, Bentz M, Speicher MR, Joos S, Ried T, Lichter P, Cremer T. Quantitative analysis of comparative genomic hybridization. *Cytometry* 1995; **19**: 27–41.
23 Rolink A, Haasner D, Nishikawa SI, Melchers F. Changes in frequencies of clonable preB cells during life in different lymphoid organs of mice. *Blood* 1993; **81**: 2290–2300.
24 Ehrlich A, Martin V, Müller W, Rajewsky K. Analysis of the B-cell progenitor compartment at the level of single cells. *Curr Biol* 1994; **4**: 573–583.
25 Kettleborough CA, Saldanha J, Ansell KH, Bendig MM. Optimization of primers for cloning libraries of mouse immunoglobulin genes using the polymerase chain reaction. *Eur J Immunol* 1993; **23**: 206–211.
26 Bentz M, Plesch A, Stilgenbauer S, Döhner H, Lichter P. Minimal sizes of deletions detected by comparative genomic hybridization. *Genes Chromosomes Cancer* 1998; **21**: 172–175.
27 Borrello MA, Phipps RP. The B/macrophage cell: an elusive link between CD5+B lymphocytes and macrophages. *Immunol Today* 1996; **17**: 471–475.
28 Ried T, Schröck E, Ning Y, Wienberg J. Chromosome painting: a useful art. *Hum Mol Genet* 1998; **7**: 1619–1626.
29 Forozan F, Karhu R, Kononen J, Kallioniemi A, Kallioniemi OP. Genome screening by comparative genomic hybridization. *Trends Genet* 1997; **13**: 405–409.
30 Yasseen AA, McKenna PG. Cytogenetic evidence for hemizygosity at the thymidine kinase locus in P388 mouse lymphoma cells. *Experientia* 1983; **39**: 532–534.
31 Demidova NS, Chernova OB, Siyanova EY, Goncharova AS, Kopnin BP. Newly formed chromosome-like structures in independent mouse P388 sublines with developed *in vivo* mdr1 gene amplification. *Somat Cell Mol Genet* 1991; **17**: 581–590.
32 Kopnin BP, Sokova OI, Demidova NS. Regularities of karyotypic evolution during stepwise amplification of genes determining drug resistance. *Mutat Res* 1992; **276**: 163–177.
33 Kinzel V, Farber B, Petrusevska RT, Fusenig N. Cytogenetic effects of phorbol ester tumor promoters: possible role in multistep tumorigenesis. *Prog Clin Biol Res* 1990; **340D**: 133–141.
34 Krishnaraju K, Hoffman B, Liebermann DA. The zinc finger transcription factor Egr-1 activates macrophage differentiation in M1 myeloblastic leukemia cells. *Blood* 1998; **92**: 1957–1966.
35 Klinken SP, Alexander WS, Adams JM. Hemopoietic lineage switch: v-raf oncogene converts Emu-myc transgenic B cells into macrophages. *Cell* 1988; **53**: 857–867.
36 Cambier N, Zhang Y, Vairo G, Kosmopoulos K, Metcalf D, Nicola NA, Elefanty AG. Expression of BCR-ABL in M1 myeloid leukemia cells induces differentiation without arresting proliferation. *Oncogene* 1999; **18**: 343–352.